

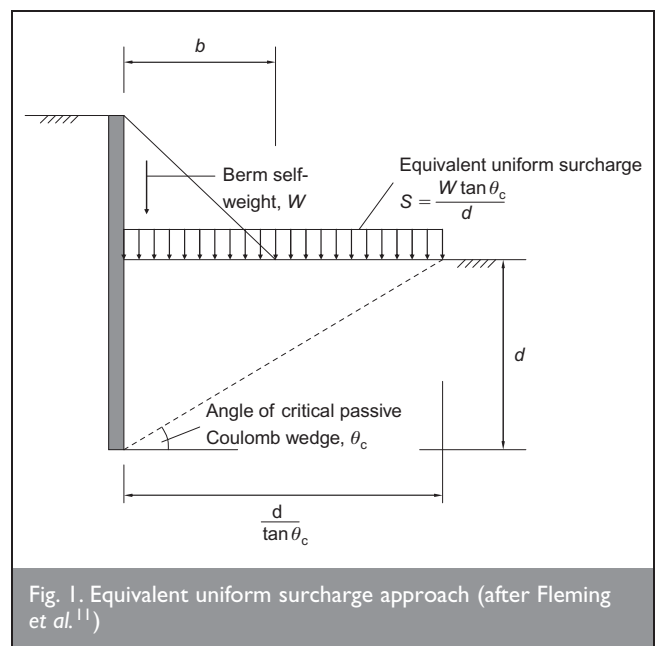
Effective-stress analysis of berm-supported retaining walls

J. A. Smethurst BEng, PhD and W. Powrie MA, MSc, PhD, CEng, FICE

Earth berms left in place against a wall during bulk excavation can provide an effective means of enhancing the stability and reducing the displacement of an embedded wall. Stability calculations for an earth berm supported wall will often need to be carried out using effective stress (rather than total stress) analysis representing long-term or drained (rather than short-term or undrained) conditions. In this paper, a multiple Coulomb wedge analysis using effective stress soil parameters is used to estimate the pressure distribution on the wall as the result of the presence of the berm. Its use in limit equilibrium wall stability calculations is compared with two commonly used empirical methods of representing a berm in such an analysis. It is shown that the raised effective formation method of representing a berm—which gives good results in an undrained or total stress analysis—is unconservative for an analysis using effective stress soil parameters, and a modified raised effective formation method is proposed.

NOTATION

b	width of base of berm
c'	cohesion component of soil strength
c_w	adhesion at soil/wall interface
d	wall embedment depth
F	lateral force acting on wall from Coulomb wedge
h	depth of excavation
l	length of potential failure surface
l_w	depth of Coulomb wedge adjacent to wall
L	depth down wall between adjacent Coulomb wedges
M	factor of safety on soil strength
N'	normal force reaction on potential failure surface
P	soil pressure acting on wall from Coulomb wedges
R_R	frictional shear resistance on failure surface
R_W	frictional shear resistance on soil/wall interface
S^*	surcharge equivalent to weight of berm (defined in Fig. 1)
U_R	pore water pressure acting on potential failure surface
U_w	pore water pressure acting on wall
W	weight of Coulomb wedge
W	weight of berm
y	increase in formation level
Z_p	depth below formation level to pivot point
β	angle of slope of ground surface
γ	unit weight of soil
γ_w	unit weight of water
δ	soil/wall friction angle



- θ angle of planar failure surface from vertical
- θ_c angle of critical planar failure surface from horizontal
- ϕ' angle of shearing resistance
- ϕ'_{crit} critical state angle of shearing resistance

1. INTRODUCTION

The perimeter walls of deep excavations for multi-level basements and highway and railway underpasses are often constructed using in situ techniques such as diaphragm walling and bored piles. Earth berms left in place against the wall during soil excavation can provide an effective means of enhancing the stability and reducing the displacement, before the permanent supports (e.g. structural basement floors, carriageway slabs and cut-and-cover tunnel roofs) are placed.

Design guidance for berms is limited, although parametric plane-strain centrifuge tests have been carried out by Powrie and Daly,¹ and finite element analyses by Clough and Denby,² Potts *et al.*,³ Carder and Bennett,⁴ Georgiadis and Anagnostopoulos,⁵ Easton *et al.*⁶ and Gourvenec and Powrie.⁷ In practice these methods are rather too specialised for routine use in design, where a limit equilibrium or basic soil–structure interaction approach (using programs such as FREW⁸ or WALLAP⁹) is commonly adopted.

Methods of representing an earth berm in limit equilibrium or soil–structure interaction calculations include the equivalent surcharge,^{10,11} the raised effective formation level¹¹ and the single Coulomb wedge approach.^{10,12} The main disadvantage of these is that the lateral resistance provided by the berm is either ignored or treated empirically and/or incorrectly. Daly and Powrie¹³ proposed a modified limit equilibrium calculation in which the distribution of passive resistance provided by the berm is represented more closely than in the methods above by using a series of Coulomb wedges over the whole depth of the wall. Their analysis was based on the undrained shear strength of the soil, and is therefore applicable only to clay soils in the short term. Daly and Powrie¹³ also showed that, of the simpler methods, the raised effective formation method was consistently the least conservative.

Stability calculations for the earth berm supported wall will often need to be carried out for long-term or drained conditions: examples include situations in which permeable soils (or bands of soil) prevent the use of an undrained approach; where the construction programme requires that the berm is left standing for a long period; or where the berm is a permanent installation. In both the model tests carried out by Powrie and Daly¹ and the finite element analyses of berm-stabilised walls carried out by Gourvenec and Powrie,⁷ the soil was allowed to swell or consolidate towards long-term equilibrium conditions. It was found that the effectiveness of the berm in reducing wall movements compared with an unsupported wall gradually increased as conditions moved from truly undrained shortly after excavation towards a long-term steady state. In some cases, the presence of the berm prevented complete collapse of the wall as the pore suctions induced by excavation dissipated.

This paper develops the multiple Coulomb wedge approach proposed by Daly and Powrie¹³ so that it can be used with effective stress soil parameters and a specified pore water pressure/suction distribution within the berm. Its use in limit equilibrium wall stability calculations is demonstrated, and a comparison is made with commonly used simpler empirical methods.

2. CURRENT METHODS OF REPRESENTING BERMS IN ANALYSIS

There are two commonly used empirical methods of representing a berm in a limit equilibrium calculation.

2.1. Equivalent uniform surcharge approach

The equivalent surcharge approach^{10,11} models the berm as an equivalent uniform surcharge S^* , added to the excavated soil surface and calculated from the weight of the berm (Fig. 1). The surcharge is applied from the wall to the edge of the critical failure surface emanating from the toe of the wall. The lateral pressure exerted by the berm is neglected.

2.2. The raised effective formation approach

The raised effective formation approach¹¹ defines a design berm geometry that has the same base width b as the actual berm but has a slope of 1:3 (Fig. 2); the maximum height of the design berm then becomes $b/3$. The design berm is modelled in the analysis by raising the formation level by half the design berm height, i.e. $b/6$. Any of the actual berm

extending above the design berm geometry (the area shown shaded in Fig. 2) can then be applied as a surcharge to the new dredge level using the equivalent surcharge approach. The lateral pressure exerted by the berm is partly modelled by this approach.

Daly and Powrie¹³ found that, in undrained conditions, the raised effective formation level approach underestimated the stability of the wall by 5–10%, and the equivalent surcharge approach by 15% when compared with their full analysis using multiple Coulomb wedges.

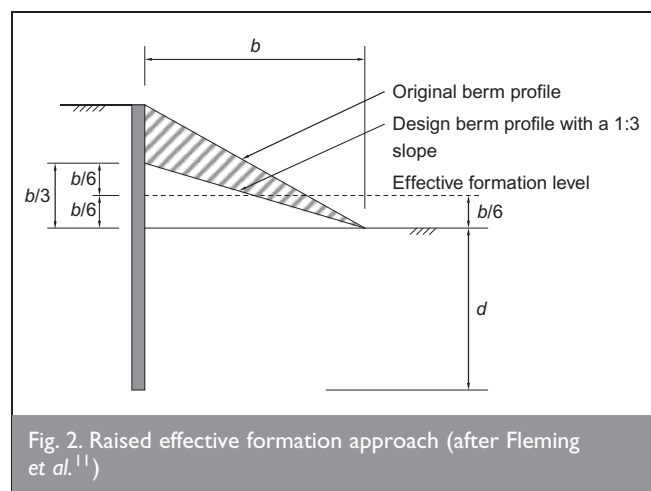
3. DRAINED LIMIT EQUILIBRIUM MULTIPLE COULOMB WEDGE ANALYSIS

3.1. Calculation of the pressure distribution and wall stability

The multiple Coulomb wedge approach¹³ uses a series of Coulomb wedges spaced at regular intervals down the wall to calculate the lateral pressure distribution from the berm. Daly and Powrie¹³ present a limit equilibrium stress analysis for berm-stabilised walls that, as well as providing an estimate of the lateral pressure exerted by the berm, enables the factor of safety on soil strength to be calculated for any given combination of berm and wall geometry and undrained soil strength properties. This analysis may be modified to use effective stress soil parameters (the frictional soil strength ϕ' , an effective cohesion c' and pore pressure u) as follows.

The effective stress resultants acting on a typical wedge are shown in Fig. 3. The distribution of passive pressure provided by the berm is calculated by carrying out Coulomb wedge analyses for a series of depths down the wall. The procedure is given below as a series of steps, and is also illustrated in Fig. 4:

- Subdivide the wall into nodes at (say) 1 m intervals over its depth.
- Assume a point of wall rotation at a depth $h + Z_p$ below original ground level. (A range of possible values for Z_p will need to be investigated.)
- Carry out a passive Coulomb wedge analysis in front of the wall at each of the nodes at and above the wall rotation



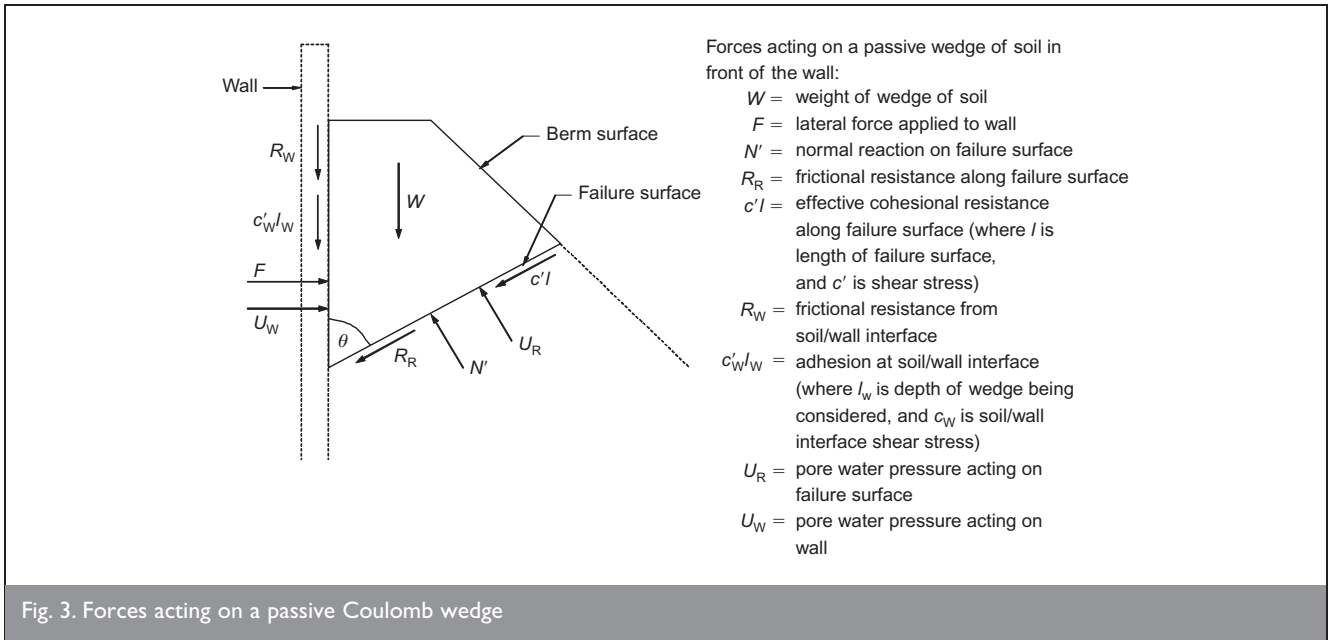


Fig. 3. Forces acting on a passive Coulomb wedge

- (pivot) point to determine the planar failure surface at each location offering the least resistance to failure.
- (d) Calculate an equivalent passive earth pressure distribution in front of the wall at and above the pivot point by dividing the difference in resistance between successive sliding wedges by the distance between adjacent nodes.
 - (e) Carry out an active Coulomb wedge analysis in front of the wall at each of the nodes at and below the pivot point to determine the planar failure surface at each location applying the largest (overturning) pressure.
 - (f) Calculate an equivalent active earth pressure distribution in front of the wall at and below the pivot point by dividing the difference in resistance between successive sliding wedges by the distance between adjacent nodes.

Behind the wall, standard active (above the pivot) and passive (below the pivot) pressures are assumed. Conventional limit equilibrium stress analyses for the wall can then be carried out, based on the fixed earth support method for cantilever walls. For a given berm geometry, wall height and depth of wall embedment, the unknown quantities are the factor of safety on soil strength (M) and the depth below the formation of the pivot point (Z_p). These can be determined using the conditions of horizontal and moment equilibrium.

3.2. Analysis of passive Coulomb wedges

Figure 3 defines the forces acting on the passive Coulomb wedge. Resolving the forces acting on the wedge vertically and horizontally gives the lateral force on the wall, F :

$$F = (N' + c'l \cot \phi') \tan \phi' \sin \theta + (N' + U_R) \cos \theta - U_w$$

where the normal reaction on the failure surface, N' , is given by

$$N' = \frac{c'l(\cos \theta + \sin \theta \tan \delta) + U_R(\cos \theta \tan \delta - \sin \theta) + W - U_w \tan \delta + c_w l_w}{\sin \theta - \tan \phi' \cos \theta - \tan \phi' \sin \theta \tan \delta - \cos \theta \tan \delta}$$

For the passive wedges at each node location, the failure surface for which F is smallest is found by trial and error by putting a range of angles θ of the failure surface from the vertical into the calculation. Corresponding equations can be determined for the active wedges below the pivot point.

The analysis in Fig. 3 assumes that the wedge failure surfaces are planar. For a wedge with a rough soil/wall interface (applied as a wall friction, δ) the most critical passive failure surfaces are curved, and the planar equivalents become unconservative.¹⁴ This is illustrated by Fig. 5, which shows the passive earth pressure coefficients for a range of wall friction ratios (δ/ϕ'), soil strengths ϕ' and slopes of the soil surface β , calculated using both a Coulomb wedge analysis with planar failure surfaces and lower-bound plasticity analysis using the equation given by Powrie¹⁵ (which gives the same result as the equations in Eurocode 7¹⁶ and CIRIA C580¹⁷). With a horizontal ground surface, the Coulomb wedges overestimate the earth pressure coefficient at ratios of $\delta/\phi' > 1/3$, for angles of friction greater than about 14° (Fig. 5(a)). For a ground surface that slopes downwards away from the wall, the Coulomb wedges slightly overestimate the earth pressure at low and high values of δ/ϕ' (Fig. 5(b)). Assuming a wall embedment d of twice the retained height h , the error in the passive pressure is between 0% and 20% for values of ϕ' less than 26° , and between about 0% and 10% for values of ϕ' less than 20° , for δ/ϕ' ratios less than $2/3$. In the analysis of the berm-supported retaining walls (the results of which are given in Tables 4–6, and are described in detail below), the values of soil strength ϕ' and the factors of safety M adopted mean that all of the multiple Coulomb wedge analyses are carried out with ϕ'_{mob} less than 21° . In comparison with the results of other methods, the factor of safety obtained from the multiple Coulomb wedge analyses may be slightly too large owing to the use of planar failure surfaces.

Daly and Powrie¹³ use zero wall friction on the passive side of wall in their undrained analyses, as in their centrifuge model tests the berms appeared to settle slightly relative to the wall (whereas wall friction relies on an upward movement of soil

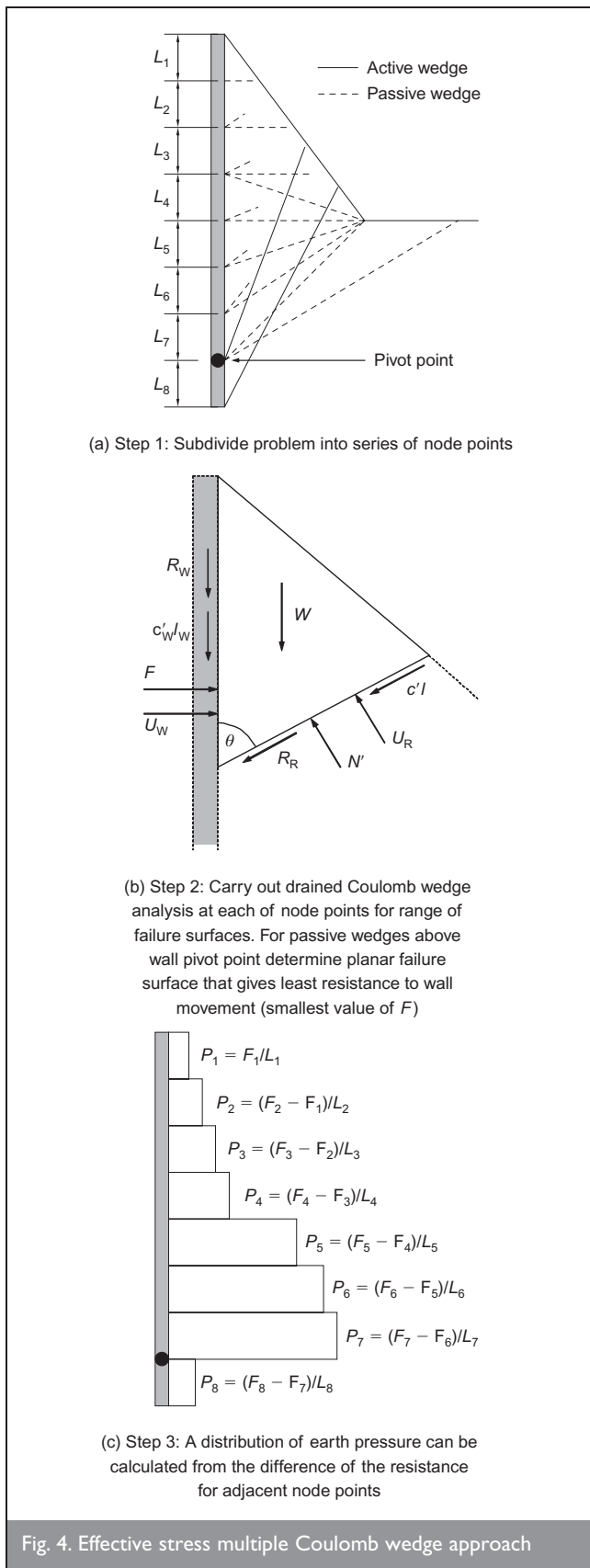


Fig. 4. Effective stress multiple Coulomb wedge approach

relative to the wall). In the long-term or drained analyses of berm-supported retaining walls, it may be overconservative to ignore wall friction: a berm-supported wall with $\delta/\phi' = 0$ may have a factor of safety only slightly larger than an equivalent unsupported cantilever wall with $\delta/\phi' = 2/3$. To investigate the influence of wall friction on the passive side, results have been calculated for a range of values of δ/ϕ' .

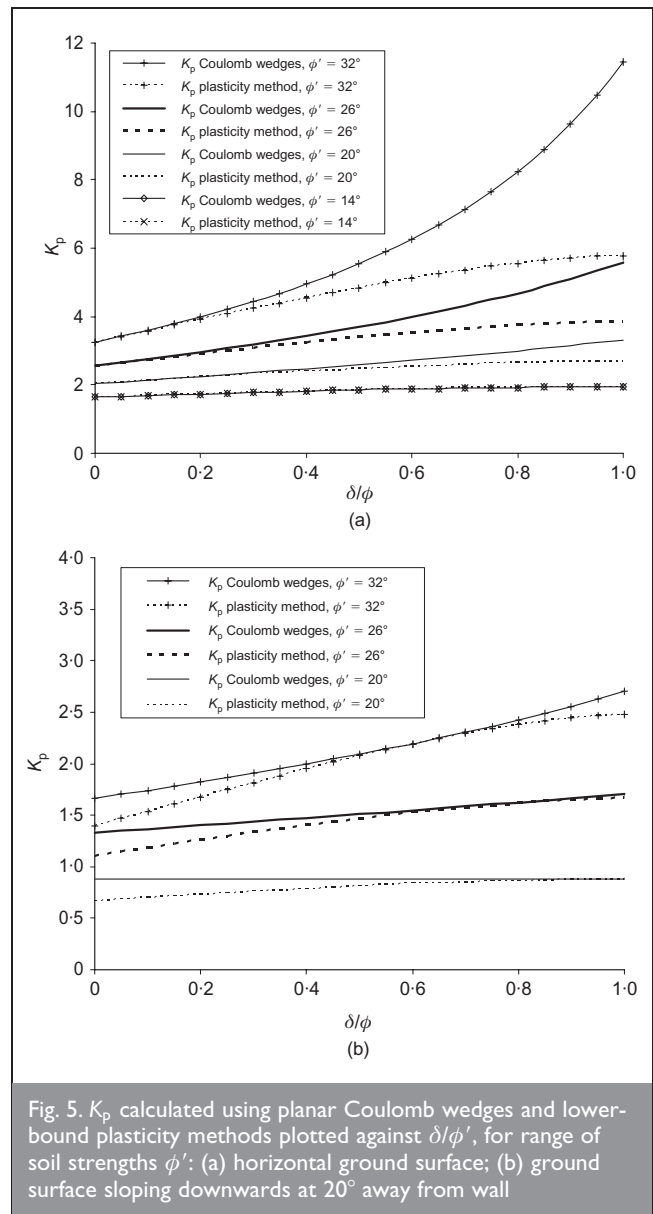


Fig. 5. K_p calculated using planar Coulomb wedges and lower-bound plasticity methods plotted against δ/ϕ' , for range of soil strengths ϕ' : (a) horizontal ground surface; (b) ground surface sloping downwards at 20° away from wall

3.3. Passive wedge (berm) stability

The multiple Coulomb wedge method of analysis considers the berm stability to some extent, in that the calculation of negative incremental values of F would indicate failure of the wedges within the berm. However, the most critical failure surface might be a circular slip passing through, for example, the crest and toe of the sloping part of the berm, and this should be checked independently by means of a limit equilibrium slope stability calculation.

The stability of the berm (and individual wedges within it) will be heavily influenced by the pore water suctions generated in the berm by the removal of the adjacent ground. In the analyses in this paper, the entire berm is assumed to be in suction (the exact distribution is discussed later). Consequently, the forces U_R and U_W are always negative for failure surfaces that are contained entirely within the berm. When negative, the pore pressure force U_W acts on the back of the soil wedge in the direction towards the wall; it is also incorporated in the wall stability calculation as a force pulling on the wall in the direction of the excavation.

4. USE OF THE MULTIPLE COULOMB WEDGE METHOD IN LIMIT EQUILIBRIUM ANALYSIS OF RETAINING WALLS

Limit equilibrium analyses have been carried out on example embedded wall and berm geometries to demonstrate the advantages of using the multiple wedges method of berm analysis presented above over methods such as the equivalent surcharge and effective formation approaches. The analyses also assess the impact of berm geometry on wall stability, as long-term equilibrium (drained) conditions are approached.

The retaining wall and initial berm geometry and the soil strength parameters are based on berm-supported walls constructed in Lias Clay as part of the Batheaston bypass.¹⁸⁻²⁰ The wall and berm geometry used is shown in Fig. 6, and the soil strength parameters are given in Table 1.

The analyses determined the factor of safety for the wall, M (applied to the soil strength in accordance with CIRIA C580¹⁷), and the depth Z_p to the pivot point from dredge level. In all of the analyses, the following assumptions were made.

- (a) No allowance was made for an unplanned excavation in front of the wall or an imposed surcharge behind the wall, as would normally be required in design following EC7,¹⁶ BS 8002²¹ and CIRIA C580¹⁷.
- (b) Wall friction in front of the wall was varied between $\delta/\phi' = 0$ and $2/3$.
- (c) Wall friction on the active side was always assumed to be $\delta/\phi' = 2/3$.
- (d) Pore pressures behind the wall were assumed to increase from zero at the ground surface, with a gradient of pore pressure increase down the wall given by the linear

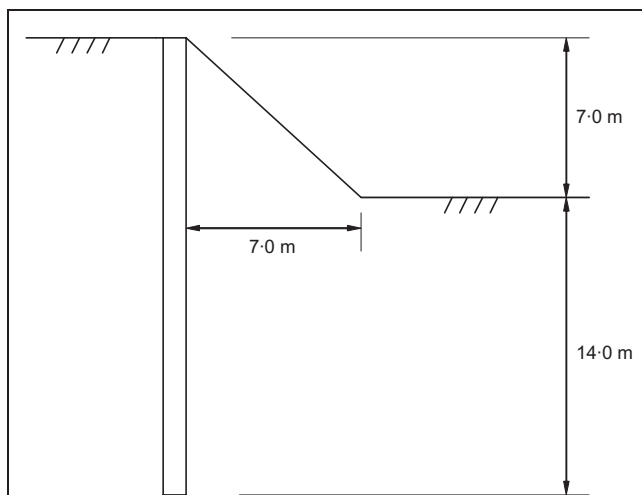


Fig. 6. Wall and berm geometry used in limit equilibrium analyses

Soil	c' : kN/m ²	ϕ' : degrees	γ : kN/m ³	γ_w : kN/m ³
Lias Clay	0	26	20	9.81

Table 1. Soil properties used in the analyses

seepage approximation assuming groundwater flow around the toe of the wall to a groundwater level at the excavated soil surface in front of the wall.

- (e) Pore pressures in front of the wall were assumed to be zero at the base of the excavation, with a gradient of pore pressure increase below this level given by the linear seepage approximation. In the calculation for the raised effective formation method, the water table was assumed to remain at the proposed excavation depth, above which the pore pressures were set to zero.
- (f) In the multiple Coulomb wedge method, pore water suctions increasing with height at the same gradient as the increase in positive pore pressures below formation level were applied within the berm. This is consistent with the limited data on long-term pore pressures in the centrifuge model tests by Powrie and Daly,¹ where suctions in the berms allowed them to remain stable. The stability of the berm may well depend on the maintenance of pore water suction, and in practice steps such as blinding the surface with a waterproof membrane to minimise any loss of suction may need to be taken. Monitoring of the suctions within the berm may also be necessary to ensure they remain large enough for continued berm stability.

5. RESULTS OF THE LIMIT EQUILIBRIUM ANALYSES

Table 2 gives the factor of safety and depth to the pivot point required for the equilibrium of the embedded cantilever wall shown in Fig. 6 with no berm, and for the same wall with a berm represented using the equivalent surcharge, raised effective formation and multiple Coulomb wedge methods, all calculated with $\delta/\phi' = 0$ on the passive side of the wall.

At an embedment depth of 14 m, the cantilever wall has a factor of safety on soil strength (M) of 0.79 and would therefore not be stable in the long term. The calculations including the berm all have factors on soil strength greater than 1.0 and demonstrate that the berm adds significant additional stability to the wall. As would be expected, the raised effective formation method provides a larger passive resistance than the equivalent surcharge method, and wall stability is therefore attained with a larger value of M . Wall stability in the multiple Coulomb wedge method is attained at values of M between those for the raised effective formation method and the equivalent surcharge method. This suggests that the raised effective formation method of representing the berm is unconservative using drained parameters, at least for the soil strength and wall and berm geometry used in this example.

Figure 7 shows the horizontal earth pressures calculated by the multiple Coulomb wedge method and raised effective formation method, in terms of both effective and total stress. The lateral total stress distribution calculated for the berm by the multiple Coulomb wedge method is negative between 2.5 and 3.5 m depth: this is because wedges at this depth in the berm are more critical than the one directly above, making the equivalent pressure $(F_{n+1} - F_n)/L_n$ negative (where F is the lateral force acting on the wall from the Coulomb wedge and L is the distance between adjacent wedges). The higher values of lateral pressure at the top of the berm are caused by the profile of suction applied (suctions increasing with height, Fig. 7(b)). The

	Cantilever wall (no berm)	Equivalent surcharge method	Raised effective formation method	Multiple Coulomb wedge method
Factor of safety (on soil strength), M	0.79	1.10	1.42	1.27
Depth to pivot point from the top of the wall, $7 + Z_p$: m	20.14	19.83	19.66	20.19

Table 2. The factor of safety and depth to the pivot point required for the stability of the wall in Fig. 6 with the berm represented in the calculation by a number of different methods

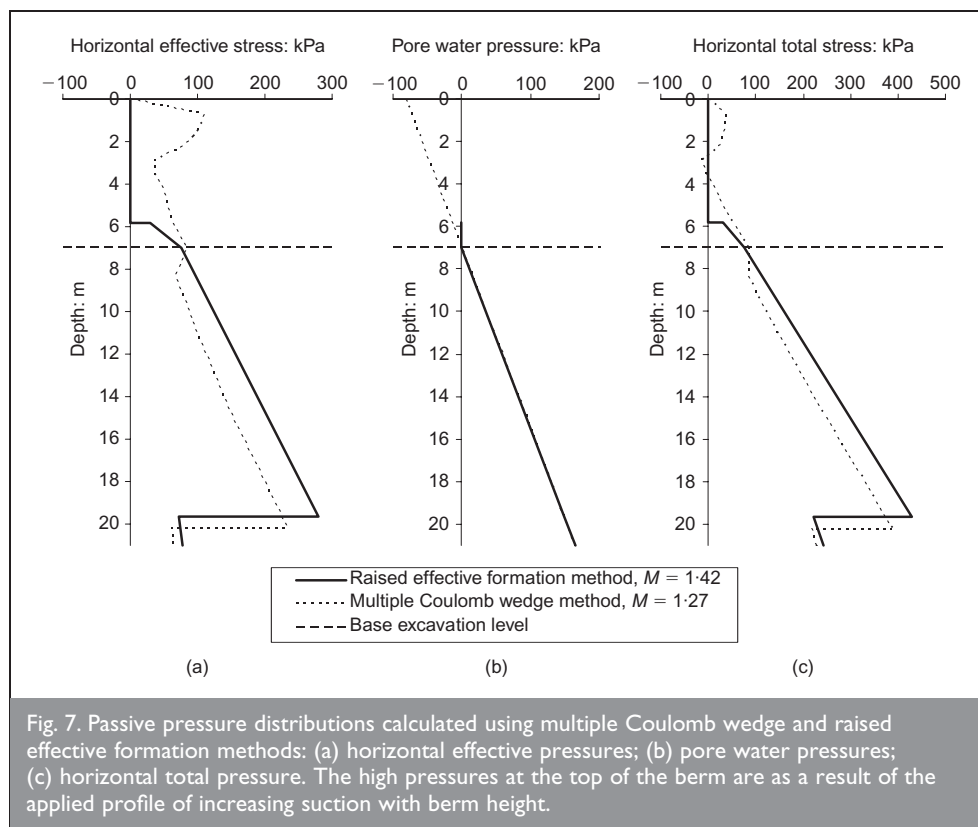


Fig. 7. Passive pressure distributions calculated using multiple Coulomb wedge and raised effective formation methods: (a) horizontal effective pressures; (b) pore water pressures; (c) horizontal total pressure. The high pressures at the top of the berm are as a result of the applied profile of increasing suction with berm height.

distribution of horizontal effective stress within the berm (Fig. 7(a)) might be considered to be unrealistic, but the distribution of horizontal total stress (Fig. 7(c)) is more plausible. Overall, the top half of the berm provides little additional stability to the wall: this may be expected with a triangular berm where the upper part becomes increasingly narrow, and is consistent with the analyses carried out by Easton *et al.*⁶ For berms that are trapezoidal in shape (including the larger berm geometry analysed later), the effect shown in Fig. 7(a) is not apparent.

method, and hence the method gives a larger passive resistance than the multiple Coulomb wedge calculation (Fig. 7).

Where the use of effective stress soil parameters requires a large wall embedment depth, the raised effective formation method will always tend to overestimate the passive resistance on the wall below the formation. This is simply because the mass of the increased volume of soil associated with the raised formation level is larger than the mass of the actual berm modelled in the multiple Coulomb wedge method. (In the

	Raised effective formation method	Multiple Coulomb wedge method
Length of failure surface from toe of wall to modelled ground surface: m	33.53	30.76
Weight of passive wedge (raised effective formation method includes weight of raised formation and UDL; multiple Coulomb wedge method includes weight of berm as defined by actual berm geometry): kN	4632	4113

Table 3. Length and weight of the passive Coulomb wedge from the toe of the wall

The reason for the larger factor of safety calculated using the raised effective formation method (when compared with the multiple wedge method) can be explained by considering the passive failure wedge from the toe of the wall and the pressure it provides to maintain wall stability. The resistance to failure of the wedge increases with the weight of the passive wedge and, if $c' > 0$, the length of the failure surface. These are shown in Table 3 for the raised effective formation method and multiple Coulomb wedge method, assuming that the failure surface emanates from the toe of the wall at an angle of 65° from vertical (this is the critical angle for the multiple Coulomb wedge method). It can be seen that the weight of the critical wedge is greater in the raised effective formation

example calculation, the failure surface from the toe of the wall reaches the modified formation level at a distance of about 30 m from the wall.) The use of greater wall friction on the passive side of the wall would probably increase the difference between the raised effective formation and multiple Coulomb wedge methods, as it will increase the size of the critical wedges.

In the undrained analyses carried out by Daly and Powrie,¹³ the multiple Coulomb wedge method consistently calculated a larger passive resistance than the raised effective formation method, because for the undrained critical wedge from the toe of the wall the increase in weight due to the actual berm is greater than the increase due to the rise in formation level. This is because of the much reduced wall depth required for stability in the undrained analyses, and because the failure surfaces form at an angle of 45° to the horizontal (compared with 45° - φ'/2 for the effective stress analysis, both assuming no wall friction).

Rather than adopt a constant increase in formation level in the raised effective formation method, a more rational approach would be to increase the level of the formation such that the weight of the associated additional volume of soil, spread over the length of the critical wedge emanating from the toe of the wall, is equal to the weight of the actual berm. For a frictionless wall, and a horizontal excavated soil surface, the increase in formation level *y* is then

3	$y = \frac{W \tan\left(45^\circ - \frac{\phi'}{2}\right)}{\gamma d}$
---	--

where *W* is the weight of the berm, *γ* is the unit weight of the soil, and *d* is the embedment depth of the wall. No further additional surcharge is applied to the formation.

Table 4 shows the factor of safety calculated for a range of berm geometries, soil strengths, wall depths and excavation depths, for different methods of representing the berm including the modified raised effective formation method represented by equation (3), all assuming δ/φ' = 0 on the passive side of the wall. In Table 4, the small berm always slopes at 45° directly from the top of the wall, as shown in Fig. 6, and the large berm geometry has a 45° slope but from a 2 m horizontal ledge at the top of the berm.

Table 4 shows that the factor of safety calculated for the original raised effective formation method is between 12% and 28% larger than for the multiple Coulomb wedge method—that is, the use in routine limit equilibrium analysis of the original raised effective formation method for the long-term effective stress case is unconservative. The equivalent surcharge method and the modified raised formation method both underestimate the stability of the wall compared with the multiple Coulomb wedge method, with factors of safety between 8% and 13% smaller for the equivalent surcharge method and 1% and 11% smaller for the modified formation method. The rise in formation level in the modified raised formation method better represents the increased height of the point of action of the resultant passive force owing to the presence of the berm. As previously discussed, the multiple Coulomb wedge method may slightly overestimate the factor of safety, owing to its use of planar (rather than curved) failure surfaces.

	Cantilever wall (no berm)	Multiple Coulomb wedge method	Equivalent surcharge method	Raised effective formation method	Modified raised formation method, equation (3)
Small berm geometry φ' = 26° Wall length = 21 m Excavation depth = 7 m	0.79	1.27	1.10 (87%)	1.42 (112%)	1.14 (89%)
Large berm geometry φ' = 26° Wall length = 21 m Excavation depth = 7 m	0.79	1.50	1.34 (89%)	1.79 (119%)	1.46 (97%)
Small berm geometry φ' = 21° Wall length = 25 m Excavation depth = 7 m	0.78	1.13	1.01 (89%)	1.30 (115%)	1.02 (90%)
Large berm geometry φ' = 21° Wall length = 25 m Excavation depth = 7 m	0.78	1.30	1.17 (90%)	1.58 (121%)	1.22 (93%)
Small berm geometry φ' = 21° Wall length = 14.5 m Excavation depth = 4 m	0.80	1.14	1.02 (89%)	1.31 (115%)	1.04 (91%)
Large berm geometry φ' = 21° Wall length = 14.5 m Excavation depth = 4 m	0.80	1.44	1.32 (92%)	1.85 (128%)	1.42 (99%)

Table 4. Factor of safety (*M*) for walls with different berm geometry, soil strength, wall embedment depth and excavation depth. Wall friction on passive side (δ/φ') = 0. The percentage in brackets is the calculated factor of safety divided by the factor of safety for the multiple Coulomb wedge method

Tables 5 and 6 show the factor of safety calculated for a range of berm geometries, soil strengths, wall depths and excavation depths, with wall friction of $\delta/\phi' = 1/3$ and $\delta/\phi' = 2/3$ on the passive side of the wall. An effect of wall friction is to make the angle of the critical planar wedge failure surface from the horizontal, θ_c , smaller than $(45^\circ - \phi'/2)$, and this was taken into account in the calculation of the increase in formation level (modified raised formation method, where θ_c replaces $45^\circ - \phi'/2$ in equation (3)) and the magnitude of the surcharge (equivalent surcharge method and raised effective formation method). The critical angle θ_c can be calculated from

$$\theta_c = -\tan^{-1} \left[\frac{\sin \delta \tan \phi' + \cos \delta \tan^2 \phi' - \sqrt{(\sin \delta \cos \delta \tan^3 \phi' + \cos^2 \delta \tan^4 \phi' + \cos^2 \delta \tan^2 \phi' + \cos \delta \sin \delta \tan \phi')}}{\cos \delta \tan \phi' + \sin \delta} \right]$$

Use of θ_c based on a planar surface with wall friction may introduce a small error, since (as discussed earlier) the actual failure surfaces of the critical wedges should be curved. A curved failure surface may give a different length from which the increase in formation is calculated, or to which the surcharge should be applied. As before, the error should be relatively small for values of mobilised friction angle ϕ'_{mob} up to about 20° , typical of clay soils.

The use of a larger wall friction angle clearly increases the factors of safety calculated, with an average increase of 12% between $\delta/\phi' = 0$ and $\delta/\phi' = 2/3$. This would generally suggest that use of zero wall friction on the passive side will lead to overly conservative designs.

Tables 5 and 6 show that for greater values of δ/ϕ' on the passive side of the wall, the raised effective formation method remains unconservative while the modified raised formation method continues to be conservative (with factors of safety 8–14% smaller than the multiple Coulomb wedge method for $\delta/\phi' = 1/3$ and 14–18% smaller for $\delta/\phi' = 2/3$). In cases in which a full calculation using the multiple Coulomb wedge method of analysis is considered too time consuming, the berm is best represented in the stability calculation for the wall using the modified raised formation method.

6. CONCLUSIONS

- A multiple Coulomb wedge analysis has been developed using effective stress parameters to show that the addition of a berm can considerably increase the stability of embedded walls in the long term.
- The use of planar failure surfaces in the multiple Coulomb wedge analysis will tend to slightly overestimate the passive resistance from the berm, since the actual critical failure surfaces should be curved. However, for values of mobilised friction angle ϕ'_{mob} typical of clay soils, the error should be relatively small (between about 0% and 10% for values of ϕ' less than 20° , and for δ/ϕ' ratios less than $2/3$).
- The original raised effective formation method should not

	Cantilever wall (no berm)	Multiple Coulomb wedge method	Equivalent surcharge method	Raised effective formation method	Modified formation method, equation (3)
Small berm geometry $\phi' = 26^\circ$ Wall length = 21 m Excavation depth = 7 m	0.91	1.39	1.18 (85%)	1.54 (111%)	1.21 (87%)
Large berm geometry $\phi' = 26^\circ$ Wall length = 21 m Excavation depth = 7 m	0.91	1.61	1.38 (85%)	1.88 (116%)	1.45 (90%)
Small berm geometry $\phi' = 21^\circ$ Wall length = 25 m Excavation depth = 7 m	0.72	1.10	0.93 (85%)	1.21 (110%)	0.95 (86%)
Large berm geometry $\phi' = 21^\circ$ Wall length = 25 m Excavation depth = 7 m	0.72	1.27	1.08 (85%)	1.48 (117%)	1.15 (90%)
Small berm geometry $\phi' = 21^\circ$ Wall length = 14.5 m Excavation depth = 4 m	0.91	1.25	1.10 (88%)	1.42 (114%)	1.11 (89%)
Large berm geometry $\phi' = 21^\circ$ Wall length = 14.5 m Excavation depth = 4 m	0.91	1.54	1.35 (88%)	1.92 (125%)	1.42 (92%)

Table 5. Factor of safety (M) for walls with different berm geometry, soil strength, wall embedment depth and excavation depth. Wall friction on passive side is $(\delta/\phi') = 1/3$. The percentage in brackets is the calculated factor of safety divided by the factor of safety for the multiple Coulomb wedge method

	Cantilever wall (no berm)	Multiple Coulomb wedge method	Equivalent surcharge method	Raised effective formation method	Modified formation method, equation (3)
Small berm geometry $\phi' = 26^\circ$ Wall length = 21 m Excavation depth = 7 m	0.99	1.51	1.22 (81%)	1.60 (106%)	1.24 (82%)
Large berm geometry $\phi' = 26^\circ$ Wall length = 21 m Excavation depth = 7 m	0.99	1.71	1.39 (81%)	1.92 (112%)	1.44 (84%)
Small berm geometry $\phi' = 21^\circ$ Wall length = 25 m Excavation depth = 7 m	0.78	1.18	0.96 (81%)	1.26 (106%)	0.97 (82%)
Large berm geometry $\phi' = 21^\circ$ Wall length = 25 m Excavation depth = 7 m	0.78	1.34	1.09 (81%)	1.51 (113%)	1.14 (85%)
Small berm geometry $\phi' = 21^\circ$ Wall length = 14.5 m Excavation depth = 4 m	0.97	1.35	1.14 (84%)	1.48 (110%)	1.15 (85%)
Large berm geometry $\phi' = 21^\circ$ Wall length = 14.5 m Excavation depth = 4 m	0.97	1.62	1.36 (84%)	1.96 (121%)	1.40 (86%)

Table 6. Factor of safety (M) for walls with different berm geometry, soil strength, wall embedment depth and excavation depth. Wall friction on passive side (δ/ϕ') = 2/3. The percentage in brackets is the calculated factor of safety divided by the factor of safety for the multiple Coulomb wedge method

be used for the analysis of wall stability in a long-term effective stress analysis, as for realistic wall embedment depths it is always unconservative. The equivalent surcharge method is, as in the short term (undrained shear strength) calculation, conservative.

- (d) A modified raised formation method for long-term effective stress analyses has been proposed that is conservative, but less so than the equivalent surcharge method. When wall friction on the passive side of the wall is invoked, the width of the passive wedge (which controls the magnitude of the rise in formation level) should be calculated taking account of the effect of wall friction in modifying the angle of the potential planar slip surface.

REFERENCES

1. POWRIE W. and DALY M. P. Centrifuge model tests on embedded retaining walls supported by earth berms. *Géotechnique*, 2002, 52, No. 2, 89–106.
2. CLOUGH G. W. and DENBY G. M. Stabilising berm design for temporary walls in clay. *Proceedings of the ASCE—Journal of the Geotechnical Engineering Division*, 1977, 103, No. GT2, 75–90.
3. POTTS D. M., ADDENBROOKE T. I. and DAY R. A. (1993). The use of soil berms for temporary support of retaining walls. In *Retaining Structures* (CLAYTON C. R. I. (ed.)). Thomas Telford, London, pp. 440–447.
4. CARDER D. R. and BENNETT S. N. *The Effectiveness of Berms and Raked Props as Temporary Support to Retaining Walls*. Transport Research Laboratory, Crowthorne, 1996, TRL Report 213.
5. GEORGIADIS M. and ANAGNOSTOPOULOS C. Effect of berms on sheet pile wall behaviour. *Géotechnique*, 1998, 48, No. 4, 569–574.
6. EASTON M. R., CARDER D. R. and DARLEY P. *Design Guidance on Soil Berms as Temporary Support for Embedded Retaining Walls*. Transport Research Laboratory, Crowthorne, 1999, TRL Report 398.
7. GOURVENEC S. M. and POWRIE W. Three-dimensional finite element analysis of embedded retaining walls supported by discontinuous earth berms. *Canadian Geotechnical Journal*, 2000, 37, No. 5, 1062–1077.
8. *FREW Version 18*. Oasis Ltd, London, 2004.
9. *WALLAP Version 5.03*. Geosolve Ltd, London, 2005.
10. PADFIELD C. J. and MAIR R. J. *Design of Retaining Walls Embedded in Stiff Clay*. Construction Industry Research and Information Association, London, 1984, CIRIA Report 104.
11. FLEMING W. G. K., WELTMAN A. J., RANDOLPH M. F. and ELSON W. K. *Piling Engineering*, 2nd edn. Blackie, Glasgow, 1992.
12. NAVFAC. *Design Manual 7.02: Foundations and Earth Structures*. US Naval Facilities Engineering Command, Alexandria, VA, 1986.
13. DALY M. P. and POWRIE W. Undrained analysis of earth berms as temporary supports for embedded retaining walls. *Proceeding of the Institution of Civil Engineers—Geotechnical Engineering*, 2001, 149, No. 4, 237–248.
14. TERZAGHI K. *Theoretical Soil Mechanics*. John Wiley, London, 1943.
15. POWRIE W. *Soil Mechanics, Concepts and Applications*, 2nd edn. Spon Press, Abingdon, 2004.

16. BRITISH STANDARDS INSTITUTION. *Eurocode 7: Geotechnical design. Part 1: General Rules*. BSI, Milton Keynes, 1995, DDENV 1997-1.
17. GABA A. R., SIMPSON B., POWRIE W. and BEADMAN D. R. *Embedded retaining walls – guidance for economic design*. Construction Industry Research and Information Association, London, 2003, CIRIA Report C580.
18. EASTON M. R. and DARLEY P. *Case History Studies of Soil Berms Used as Temporary Support to Embedded Retaining Walls*. Transport Research Laboratory, Crowthorne, 1999, TRL Report 380.
19. GOURVENEK S. M., POWRIE W., LACY M. and STEVENSON M. Observation of diaphragm wall movements in Lias Clay during construction of the A4/A46 bypass in Bath, Avon. In *Geotechnical Aspects of Underground Construction in Soft Ground* (MAIR R. J. and TAYLOR R. N. (eds)). Balkema, Rotterdam, 1996, pp. 143–147.
20. GOURVENEK S. M. *Three Dimensional Effects of Diaphragm Wall Installation and Staged Construction Sequences*. PhD thesis, University of Southampton, 1998.
21. BRITISH STANDARDS INSTITUTION. *Code of Practice for Earth Retaining Structures BS8002, incorporating Amendments Nos. 1 and 2 and Corrigendum No. 1*. British Standards Institution, Milton Keynes, 2001.

What do you think?

To comment on this paper, please email up to 500 words to the editor at journals@ice.org.uk

Proceedings journals rely entirely on contributions sent in by civil engineers and related professionals, academics and students. Papers should be 2000–5000 words long, with adequate illustrations and references. Please visit www.thomastelford.com/journals for author guidelines and further details.